

Electronic Supplementary Information

Framework Al Zoning in Zeolite ECR-1

Jiho Shin,^a Nak Ho Ahn,^a Sung June Cho,^b Limin Ren,^c Feng-Shou Xiao,^c and Suk Bong Hong^{*a}

^a Centre for Ordered Nanoporous Materials Synthesis, School of Environmental Science and Engineering and Department of Chemical Engineering, POSTECH, Pohang 790-784, Korea

^b Department of Applied Chemical Engineering, Chonnam National University, Kwangju 500-757, Korea

^c Department of Chemistry, Zhejiang University, Hangzhou 310028, P. R. China

Zeolite Synthesis. The as-made Na⁺ form (Na-ECR-1) of ECR-1 with Si/Al = 3.5 was synthesized under wholly inorganic conditions following the procedures reported by Song *et al.*^{S1} The Sr²⁺- and La³⁺-exchanged forms (Sr-ECR-1 and LaNa-ECR-1, respectively) of ECR-1 were prepared by stirring Na-ECR-1 twice in 1.0 M Sr(NO₃)₂ and 0.1 M La(NO₃)₃ solutions at 80 °C for 6 h, respectively. A mazzite-type zeolite (i.e., zeolite omega) with Si/Al = 3.2 was prepared in the presence of tetramethylammonium and Na⁺ ions according to the procedure of Jarman *et al.*,^{S2} calcined under flowing air at 550 °C for 8 h to remove the occluded organic species, and then converted to its Na⁺ form (Na-MAZ) by stirring twice in 1.0 M NaNO₃ solutions at 80 °C for 6 h. The proton form (JRC-Z-HM10) of mordenite with Si/Al = 5.0 was obtained from the Catalysis Society of Japan and converted to its Na⁺ form (Na-MOR) following the procedure given above.

Structural Analysis. The high-resolution synchrotron X-ray diffraction (XRD) patterns for Na-ECR-1, Sr-ECR-1, and LaNa-ECR-1 in dehydrated state were collected at 300 °C in capillary mode on the RIKEN materials science BL44B2 beamline at the SPring-8 (Harima, Japan) using a monochromated X-ray ($\lambda = 0.5000 \text{ \AA}$). A large Debye-Scherrer camera with a camera length of 286.48 mm was used with an imaging plate as a detector, and all diffraction

patterns were obtained with a 0.01 degree step in 2θ . The samples were loaded into 0.5 mm quartz glass capillaries, heated from room temperature to 300 °C at a ramping rate of 10 °C min⁻¹, and kept at the same temperature for 10 min. Then, the capillaries were sealed with beeswax and rotated during the measurements (20 min of irradiation). When we again obtained the XRD measurements on ECR-1 under the same measurement conditions, we were able to observe no noticeable differences in the intensity of X-ray reflections, suggesting that no significant structural collapse was caused during the XRD measurements. The high-resolution synchrotron XRD data for Na-MAZ and Na-MOR were collected on the 9B beamline at equipped with a ceramic furnace of the Pohang Acceleration Laboratory (Pohang, Korea) using monochromated X-rays ($\lambda = 1.5472 \text{ \AA}$). The detector arm of the vertical scan diffractometer consists of seven sets of Soller slits, flat Ge(111) crystal analyzers, anti-scatter baffles, and scintillation detectors, with each set separated by 20°. Data were obtained on the sample at room temperature in flat plate mode, with a step size of 0.015° and overlaps of 2° to the next detector bank over the 2θ range 10-131°.

The structures obtained in this work were refined via the Rietveld method using the GSAS suite of programs and EXPGUI graphical interface,^{S3} with soft restraints applied to T-O and O-O distances in the tetrahedral framework (1.65 and 2.65 Å, respectively). Peak shape was modeled using the pseudo-Voigt profile function.^{S4} Si and Al atoms were positioned on each tetrahedral site (T-site) with fractional occupancies estimated from the bulk Si/Al ratio, assuming that the Al atoms were disordered over all T-sites. The extraframework cations were located via Fourier difference maps. Difference Fourier peaks located at reasonable distances from the framework were investigated as possible sites by refinement of occupancy and position. The locations of Na⁺ ions in Na-MAZ and Na-MOR were found to be in good agreement with the reported positions of the same cations in omega and mordenite, respectively.^{S5}

(S1) J. Song, L. Dai, Y. Ji, F.-S. Xiao, *Chem. Mater.*, 2006, **18**, 2775.

(S2) R. Jarman, A. Jacobson, M. Melchior, *J. Phys. Chem.*, 1984, **88**, 5748.

(S3) (a) H. M. Rietveld, *J. Appl. Crystallogr.*, 1969, **2**, 65. (b) A. Larson, R. B. von Dreele, *General Structure Analysis System GSAS*; Los Alamos National Laboratory: Los Alamos, NM, 2000. (c) B. H. Toby, *J. Appl. Crystallogr.*, 2001, **34**, 210.

(S4) J. B. Hastings, W. Thominson, D. E. Cox, *J. Appl. Crystallogr.*, 1984, **17**, 85.

(S5) (a) E. Galli, *Cryst. Struct. Comm.*, 1974, **3**, 339. (b) A. Martucci, A. Alberti, M. D. Guzman-Castillo, F. Di Renzo, F. Fajula, *Microporous Mesoporous Mater.*, 2003, **63**, 33. (c) W. M. Meier, *Z. Kristallogr.*, 1961, **115**, 439.

Table S1 Agreement factors for Rietveld refinement for zeolites studied here

Parameter	Na-MAZ	Na-ECR-1	Sr-ECR-1	LaNa-ECR-1	Na-MOR
$R(F^2)$, number of observations	9.86%, 461	12.96%, 3088	14.88%, 3744	13.77%, 2424	7.16%, 825
χ^2 , number of refined variables	6.470, 79	8.100, 89	4.713, 108	5.162, 103	9.655, 64
R_{wp}	6.05%	2.79%	1.92%	2.49%	6.52%
R_p	4.09%	2.02%	1.27%	1.80%	4.59%

Table S2 Final atomic coordinates and thermal parameters for Na-ECR-1

Atom	<i>x</i>	<i>y</i>	<i>z</i>	<i>U</i> _{iso} (x 100 Å ²)
T1	-0.25	0.1626(6)	-0.0061(5)	3.27(8)
T2	-0.25	0.0762(8)	0.0999(6)	3.27(8)
T3	-0.25	0.1624(5)	0.2072(6)	3.27(8)
T4	0.0422(11)	0.1630(5)	-0.0930(4)	3.27(8)
T5	0.0486(12)	-0.0203(5)	0.1461(5)	3.27(8)
T6	0.0422(12)	0.0573(5)	0.2493(5)	3.27(8)
T7	0.25	0.1638(6)	0.3937(6)	3.27(8)
T8	0.25	0.1651(6)	0.5168(5)	3.27(8)
T9	-0.0428(11)	0.0530(5)	0.3620(5)	3.27(8)
T10	0.0429(12)	-0.0508(5)	0.4519(4)	3.27(8)
O1	-0.25	0.25	0.0147(9)	3.68(17)
O2	-0.25	0.1069(9)	0.0415(5)	3.68(17)
O3	-0.25	0.1441(10)	0.1438(5)	3.68(17)
O4	-0.25	0.25	0.2173(13)	3.68(17)
O5	-0.0729(13)	0.1473(8)	-0.0403(5)	3.68(17)
O6	-0.0688(14)	0.0270(7)	0.1060(6)	3.68(17)
O7	-0.0713(14)	0.1265(6)	0.2338(6)	3.68(17)
O8	0.0209(31)	0.25	-0.1143(10)	3.68(17)
O9	0.0006(26)	-0.0049(8)	0.2073(6)	3.68(17)
O10	0.25	0.1377(12)	-0.0858(10)	3.68(17)
O11	0.25	0.0126(11)	0.1327(12)	3.68(17)
O12	0.25	0.0838(12)	0.2546(11)	3.68(17)
O13	-0.0476(21)	0.1085(6)	-0.1399(6)	3.68(17)
O14	-0.0062(23)	0.0171(8)	0.3035(5)	3.68(17)
O15	0.25	0.25	0.3747(10)	3.68(17)
O16	0.25	0.25	0.5323(12)	3.68(17)
O17	0.25	0.1537(10)	0.4538(4)	3.68(17)
O18	0.0736(13)	0.1253(6)	0.3675(6)	3.68(17)
O19	0.0700(14)	0.1273(6)	0.5430(6)	3.68(17)
O20	0.0102(24)	-0.0107(8)	0.3994(5)	3.68(17)
O21	0	0	0.5	3.68(17)
O22	-0.25	0.0874(12)	0.3659(12)	3.68(17)
O23	-0.25	0.0867(11)	0.5416(11)	3.68(17)

Table S3 Final atomic coordinates and thermal parameters for Sr-ECR-1

Atom	x	y	z	U_{iso} (x 100 Å ²)
T1	0.25	0.1637(3)	0.5047(3)	2.96(13)
T2	0.25	0.0772(4)	0.3977(3)	2.96(13)
T3	0.25	0.1631(3)	0.2934(3)	2.96(13)
T4	0.0453(7)	0.6652(3)	0.4115(3)	2.96(13)
T5	0.0445(7)	0.0246(4)	0.6467(3)	2.96(13)
T6	0.5438(7)	0.0581(4)	0.2507(3)	2.96(13)
T7	0.25	0.6635(3)	0.8935(3)	2.96(13)
T8	0.25	0.6636(3)	0.0152(3)	2.96(13)
T9	0.0436(7)	0.0517(4)	0.1397(4)	2.96(13)
T10	0.5445(7)	0.5522(4)	0.0465(2)	2.96(13)
O1	0.25	0.25	0.4909(4)	2.71(25)
O2	0.25	0.1133(4)	0.4540(3)	2.71(25)
O3	0.25	0.1430(7)	0.3543(3)	2.71(25)
O4	0.25	0.25	0.2847(7)	2.71(25)
O5	0.0755(5)	0.1436(4)	0.5393(3)	2.71(25)
O6	0.0592(9)	0.0334(5)	0.3892(4)	2.71(25)
O7	0.0748(5)	0.1269(3)	0.2664(3)	2.71(25)
O8	0.493(4)	0.25	0.6052(5)	2.71(25)
O9	0.5151(16)	-0.0083(4)	0.2927(3)	2.71(25)
O10	0.25	0.6373(15)	0.4237(7)	2.71(25)
O11	0.25	0.4688(13)	0.6322(7)	2.71(25)
O12	0.25	0.5795(9)	0.7525(9)	2.71(25)
O13	0.0244(17)	0.1132(4)	0.6375(3)	2.71(25)
O14	0.0271(18)	0.0192(5)	0.1986(3)	2.71(25)
O15	0.25	0.75	0.8814(7)	2.71(25)
O16	0.25	0.75	0.0257(5)	2.71(25)
O17	0.25	0.6456(7)	0.9537(3)	2.71(25)
O18	0.0834(8)	0.6260(4)	0.0477(4)	2.71(25)
O19	0.5754(5)	0.1255(3)	0.1341(3)	2.71(25)
O20	0.5250(11)	0.5108(4)	0.1011(2)	2.71(25)
O21	0	0	0	2.71(25)
O22	0.25	0.0830(5)	0.9584(4)	2.71(25)
O23	0.25	0.0715(7)	0.1287(7)	2.71(25)

Table S4 Final atomic coordinates and thermal parameters for LaNa-ECR-1

Atom	<i>x</i>	<i>y</i>	<i>z</i>	<i>U</i> _{iso} (x 100 Å ²)
T1	-0.25	0.1622(5)	-0.0086(5)	2.90(10)
T2	-0.25	0.0744(8)	0.0973(5)	2.90(10)
T3	-0.25	0.1636(5)	0.2027(6)	2.90(10)
T4	0.0465(10)	0.1629(4)	-0.0897(5)	2.90(10)
T5	0.0492(11)	-0.0194(6)	0.1441(5)	2.90(10)
T6	0.0485(11)	0.0657(5)	0.2455(4)	2.90(10)
T7	0.25	0.1627(5)	0.3924(6)	2.90(10)
T8	0.25	0.1632(5)	0.5162(5)	2.90(10)
T9	-0.0423(11)	0.0515(6)	0.3586(5)	2.90(10)
T10	0.0459(11)	-0.0514(5)	0.4522(4)	2.90(10)
O1	-0.25	0.25	0.0017(9)	3.17(20)
O2	-0.25	0.1156(7)	0.0437(4)	3.17(20)
O3	-0.25	0.1270(8)	0.1462(4)	3.17(20)
O4	-0.25	0.25	0.1939(10)	3.17(20)
O5	-0.0761(11)	0.1387(7)	-0.0413(4)	3.17(20)
O6	-0.0737(12)	0.0191(7)	0.1000(6)	3.17(20)
O7	-0.0761(12)	0.1384(6)	0.2355(5)	3.17(20)
O8	0.0321(29)	0.25	-0.1023(9)	3.17(20)
O9	0.0172(26)	0.0075(7)	0.2000(4)	3.17(20)
O10	0.25	0.1387(11)	-0.0766(9)	3.17(20)
O11	0.25	-0.0013(11)	0.1251(10)	3.17(20)
O12	0.25	0.0972(11)	0.2458(10)	3.17(20)
O13	-0.0259(19)	0.1116(5)	-0.1380(5)	3.17(20)
O14	0.0034(23)	0.0252(8)	0.2991(4)	3.17(20)
O15	0.25	0.25	0.3767(8)	3.17(20)
O16	0.25	0.25	0.5290(8)	3.17(20)
O17	0.25	0.1510(9)	0.4543(4)	3.17(20)
O18	0.0755(12)	0.1251(5)	0.3670(6)	3.17(20)
O19	0.0753(12)	0.1263(6)	0.5438(6)	3.17(20)
O20	0.0102(24)	-0.0123(7)	0.3977(5)	3.17(20)
O21	0	0	0.5	3.17(20)
O22	-0.25	0.0766(13)	0.3616(12)	3.17(20)
O23	-0.25	0.0799(11)	0.5463(10)	3.17(20)

Table S5 Final atomic coordinates and thermal parameters for Na-MAZ

Atom	<i>x</i>	<i>y</i>	<i>z</i>	<i>U</i> _{iso} (x 100 Å ²)
T1	0.09318(11)	0.35541(11)	0.04584(24)	1.976(29)
T2	0.48951(17)	0.15666(16)	0.25	1.976(29)
O1	0	0.27609(30)	0	2.58(6)
O2	0.11106(21)	0.43711(20)	0.9283(4)	2.58(6)
O3	0.16329(17)	0.32646(33)	0.0018(7)	2.58(6)
O4	0.09662(33)	0.38322(30)	0.25	2.58(6)
O5	0.5149(5)	0.25739(25)	0.25	2.58(6)
O6	0.57841(23)	0.1569(5)	0.25	2.58(6)

Table S6 Final atomic coordinates and thermal parameters for Na-MOR

Atom	x	y	z	U_{iso} (x 100 Å ²)
T1	0.30321(21)	0.07341(16)	0.0379(5)	1.771(27)
T2	0.30338(19)	0.31140(21)	0.0378(5)	1.771(27)
T3	0.08786(26)	0.38213(28)	0.25	1.771(27)
T4	0.08383(27)	0.22561(25)	0.25	1.771(27)
O1	0.2742(5)	0	0	3.74(7)
O2	0.3309(5)	0.0764(5)	0.25	3.74(7)
O3	0.37590(32)	0.08687(31)	0.9336(8)	3.74(7)
O4	0.23804(32)	0.12222(34)	1.0038(12)	3.74(7)
O5	0.3301(5)	0.3118(6)	0.25	3.74(7)
O6	0.25	0.25	0	3.74(7)
O7	0.37405(29)	0.3082(4)	0.9282(7)	3.74(7)
O8	0	0.4068(6)	0.25	3.74(7)
O9	0.0906(5)	0.3038(4)	0.25	3.74(7)
O10	0	0.1964(8)	0.25	3.74(7)

Table S7 Refined Na⁺ positions and occupancies in Na-MAZ, Na-ECR-1, and Na-MOR zeolites

Material	Site	x	y	z	Occupancy	Multiplicity	U_{iso} (x 100 Å ²)	Na ⁺ /maz layer	Na ⁺ /mor layer
Na-MAZ	A	0.0780(7)	0.5391(4)	0.25	0.937(8)	6	27.5(4)	5.622	-
	E	0.1635(12)	0.0817(6)	0.25	0.441(6)	6	27.5(4)	2.646	-
	F	0.6667	0.3333	0.25	0.320(12)	2	27.5(4)	0.640	-
Na-ECR-1	A	0	0	0	1 (capped)	4	9.8(8)	4.000	-
	B	0.584(4)	0.25	0.3076(11)	0.947(11)	4	9.8(8)	1.894	1.894
	C	0.25	0.75	0.4023(24)	0.768(22)	2	9.8(8)	-	1.536
	D	0.75	0.5763(16)	0.2615(15)	0.905(17)	4	9.8(8)	3.620	-
	E	0.25	0.75	0.223(4)	0.427(20)	2	9.8(8)	0.854	-
	F	0.75	0.25	0.1103(24)	0.839(21)	2	9.8(8)	1.678	-
Na-MOR	B	0.50	0	0	0.365(10)	4	25.8(6)	-	1.460
	C	0.50	0.3415(13)	0.25	0.730(12)	4	25.8(6)	-	2.920
	D	0.1739(16)	-0.0093(23)	0.25	0.420(8)	8	25.8(6)	-	3.360

Table S8. Refined Sr²⁺ positions in Sr-ECR-1

Site	x	y	z	Occupancy	Multiplicity	U_{iso} (x 100 Å ²)	Sr ²⁺ /maz layer	Sr ²⁺ /mor layer
A	0	0	0.5	0.555(8)	4	6.1(4)	2.220	-
B	-0.0324(27)	0.25	0.1968(7)	0.536(5)	4	6.1(4)	1.072	1.072
B'	0.26(8)	0.25	0.1377(20)	0.159(4)	4	6.1(4)	-	0.636
C	0.674(5)	0.75	0.0799(16)	0.256(5)	4	6.1(4)	-	1.024
D	0.25	0.5965(14)	0.2527(14)	0.362(7)	4	6.1(4)	1.448	-
G	0.75	0.150(5)	0.328(4)	0.112(6)	4	6.1(4)	0.448	-

Table S9 Refined La^{3+} and Na^+ positions in LaNa-ECR-1

Site	x	y	z	Occupancy	Multiplicity	U_{iso} (x 100 Å ²)	Cation/maz layer	Cation/mor layer
A	0	0	0	0.266(5)	4	8.4(4)	1.064 (La^{3+})	-
B	0.4939(23)	0.25	0.3098(5)	0.414(25)	4	8.4(4)	0.828 (La^{3+})	0.828 (La^{3+})
C	0.75	0.248(22)	0.5650(27)	0.427(10)	4	8.4(4)	-	1.708 (Na^+)
D	-0.146(5)	0.5491(15)	0.2476(16)	0.622(4)	8	8.4(4)	4.976 (Na^+)	-
E	0.75	0.75	0.2635(26)	0.150(5)	2	8.4(4)	0.300 (La^{3+})	-

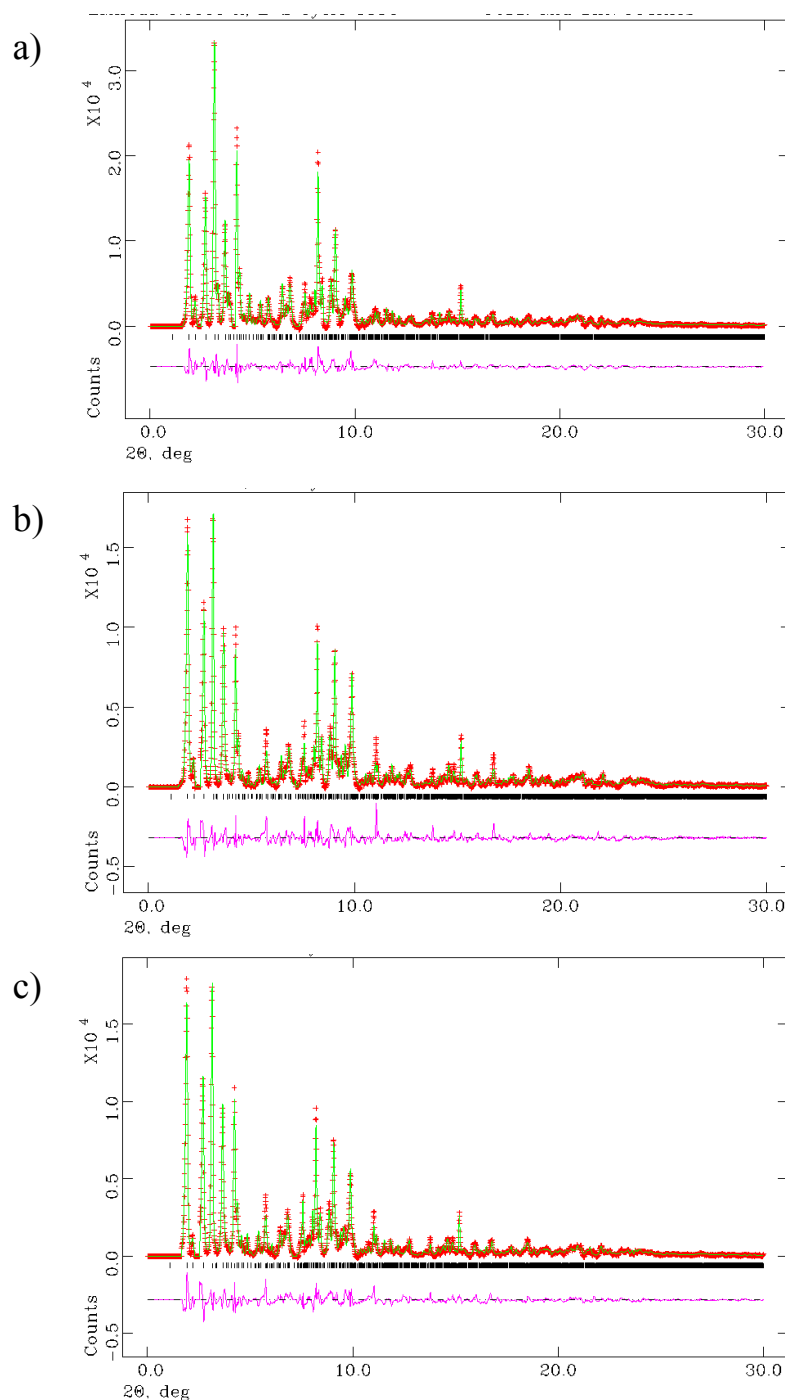


Fig. S1. Rietveld plots for (a) Na-ECR-1, (b) Sr-ECR-1, and (c) LaNa-ECR-1: observed (crosses), calculated (solid line), and difference (lower trace) synchrotron powder XRD patterns. The tick marks indicate the positions of allowed reflections.

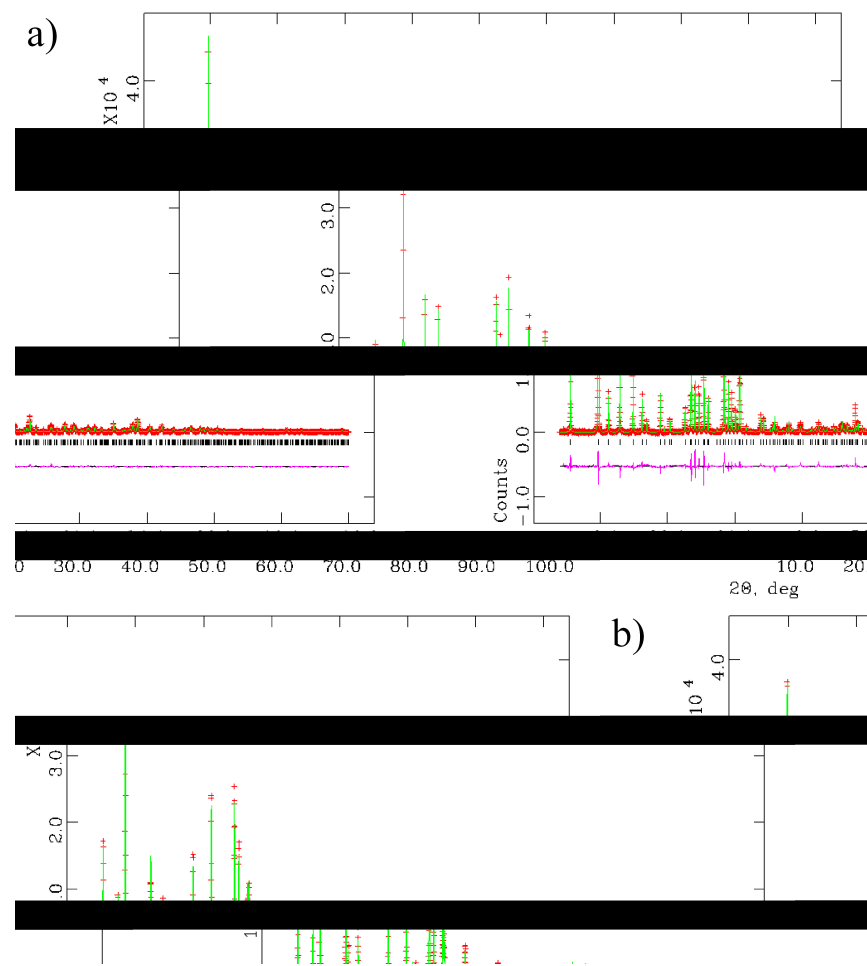


Fig. S2. Rietveld plots for (a) Na-MAZ, and (b) Na-MOR: observed (crosses), calculated (solid line), and difference (lower trace) synchrotron powder XRD patterns. The tick marks indicate the positions of allowed reflections.

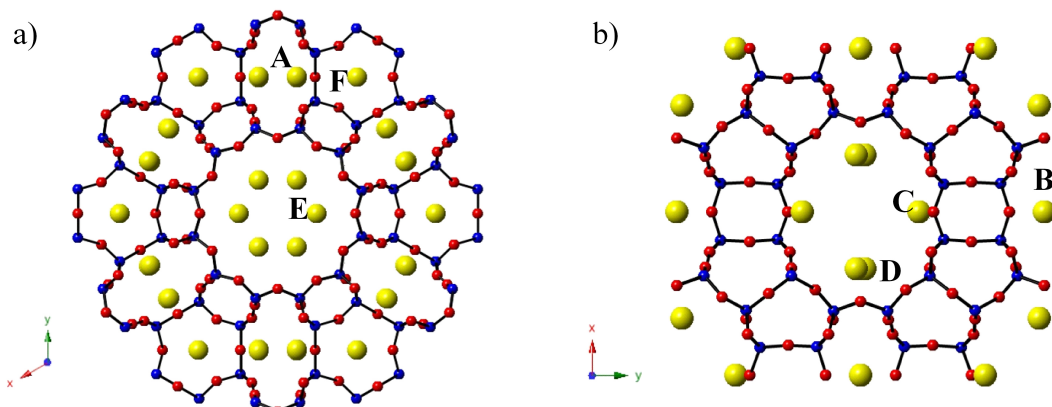


Fig. S3. Refined Na^+ cation sites in (a) Na-MAZ and (b) Na-MOR.